ISSN 1392-1320 MATERIALS SCIENCE (MEDŽIAGOTYRA). Vol. XX, No. X. 2026

B_2O_3 Induced Zinc Tungstate-epoxy Composite for High Performance Antenna Applications

Lamees Salam FAEQ

College of Materials Engineering, University of Technology-Iraq, Alsina'a Street, 10066 Baghdad, Iraq

http://doi.org/10.XXXX/j01.xxxxxxx

Received 2 February 2026; accepted 3 April 2026

Microwave dielectric ceramics, dispersed polymer matrix composites, play a pivotal role in contemporary wireless communication systems due to the strategic combination of miniaturization and efficient electromagnetic wave processing. In this work, complex oxides were prepared to suit the requirements of compact and superior high-frequency devices. The zinc tungstate-boron oxide and zinc tungstate powders were synthesised by a solid-state reaction and subsequently embedded in an epoxy matrix to provide a new functional polymer composite. Structural characterizations were measured with x-ray diffraction (XRD (Lab6000)), and microwave dielectric properties were measured with a Vector Network Analyser (VNA). The resulting zinc tungstate – 5 wt.% boron oxide/epoxy composite showed great potential dielectric performance with a high dielectric constant (ε_r) of 30 and a low loss tangent (tan δ) of 0.0001. To illustrate the practical feasibility of these composites, Computer Simulation Technology (CST) Studio Suite was used to design and simulate a microstrip patch antenna. Simulation results revealed that incorporating 5 % boron oxide not only improved the microwave dielectric properties but also transformed the material into a highly effective antenna substrate that surpasses traditional materials with respect to matching depth (-45 dB) and radiation efficiency (93.4 %).

Keywords: microwave dielectric composites, CST Studio Suite, loss tangent, dielectric constant.

1. INTRODUCTION

Microwave dielectric materials are vital for modern wireless communication systems such as resonators, antennas, filters, and dielectric substrates. These materials are fundamental for applications like GPS (Global Positioning Systems), mobile communications, and various advanced wireless technologies [1 – 4]. Wolframite (zinc tungstate) structures have garnered significant interest in microwave applications due to their good dielectric properties [5]. Boron oxide (B_2O_3) is a generally used additive in microwave dielectric ceramic systems, known for reducing loss factor, enhancing material flexibility, and improving structural uniformity. Several researchers have investigated the effect of boron addition on microwave dielectric characterisation of ceramics. For instance, Wang et al. prepared microwave ceramics using a Li_2CO_3: Al_2O_3: H_3BO_3 system, achieving good dielectric characteristics (ε_r ~ 3.2 – 3.9, $Q \times f$ ~ 21.500 – 35.500 GHz, τ_f ~ −52 to −64 ppm/°C) [6]. Similarly, Zhou et al. showed that blending H_3BO_3 with Bi_2O_3 enabled the sintering process at under 650 °C with an εr of about 12.14, a $Q \times f$ of around 14.800 GHz, and a τ_f of roughly −72 ppm/°C. Also prepared a special glass composite, CuO-ZnO-B_2O_3-Li_2O/Al_2O_3, using a solid-state reaction. This was for ULTCC applications and worked well with Ag and Al electrodes at 640 °C [7]. Additionally, Zhou et al. reported high-performance $LiBO_2$-H_3BO_3-B_2O_3-Li_2CO_3 microwave ceramics sintered at 640°C with ε_r ~ 5.95, $Q \times f$ ~ 41,800 GHz, and τ_f ~ −72 ppm/°C. Studies on pure H_3BO_3 ceramics showed promising results. Pang et al. synthesized H_3BO_2 ceramics by low-temperature dehydration at 190 °C (ε_r ~ 2.12, $Q \times f$ ~ 32,700 GHz, τ_f ~ −43 ppm/°C) [8]. Ding et al. prepared high-performance H_3BO_3 ceramics using dry pressing at room temperature. These ceramics had great properties (ε_r ~ 2.78 – 2.89), ($Q \times f$ ~ 56,900 – 59,400GHz), and stable temperature behavior (τ_f ~ −91 to −95.5 ppm/°C). [9]. Li and others found that microwave dielectric properties of H_3BO_3 ceramics (ε_r ~ 2.84, $Q \times f$ ~ 146.000 GHz, τ_f ~ −242 ppm/°C). However, $Q \times f$ values decreased significantly from 146.000 GHz to 75.000 GHz after 24 hours in air due to the high moisture absorption of H_3BO_3, which remains a key challenge in borate-based microwave ceramics [10]. Recent studies emphasised the continuous evolution of tungstate-based ceramics for high-frequency applications. For instance, recent illustrations of zinc tungstate materials have demonstrated that sintering can substantially refine grain boundaries, thereby enhancing dielectric stability [11]. Additionally, the role of boron-based additives has been re-examined in 2024, where B_2O_3 was found to not only act as a sintering aid but also to minimize the loss tangent by stabilising the crystal lattice against defects and moisture [12]. While several polymer-ceramic composites have been proposed for 5G substrates recently [13], the synergistic effect of B_2O_3 modification specifically within a zinc tungstate-epoxy composite remains underexplored in existing literature. This lack of work represents a role knowledge gap, as understanding this interaction is important for developing high-performance composites for microwave applications. Therefore, this work aims to bridge this gap by exploring the effect of boron oxide addition on the microwave dielectric properties of composites. A key objective is the preparation of polymer-ceramic composites to achieve a high-performance material

* Corresponding author: L.S. Faeq
E-mail: *130205@uotechnology.edu.iq*

with cost effectiveness and ease of processing. By dispersing the synthesized powders into an epoxy matrix, we sought to develop a composite suitable for flexible electronic applications while the ceramic materials were synthesized using the solid-state reaction process. X-ray diffraction (XRD) analysis was conducted to confirm phase formation, and the dielectric properties were evaluated using a vector network analyzer (VNA) were converted into dielectric properties, including dielectric constant and loss tangent, using the well-known Nicolson-Ross-Weir (NRW) mathematical model.

To bridge the gap between the development of materials and device implementation, CST Studio Suite was used to simulate and design antennas using the experimentally characterized dielectric composite materials. Initially, CST studio suite was used to model unit-cell structures to predict effective permittivity and permeability, verifying the numerical results against measured data [14].

2. EXPERIMENTAL PROCEDURE

Zinc tungstate and zinc tungstate-boron oxide (0 and 5 wt.%) ceramics were prepared using a solid-state reaction route. The starting materials, ZnO (99 %) and WO_3 (99 %) were taken in the appropriate proportion and B_2O_3-doped was varied up to 5 % wt. respectively. The materials were milled and blended for six hours, then heated the mixture at 900 °C for six hours. After that, the results samples were re-milled for another six hours. Finally, the composite specimens were prepared by a manual mixing technique of the synthesized complex oxides with the epoxy matrix. To ensure a void-free structure, the mixture was subjected to an ultrasonication treatment to eliminate air bubbles. Subsequently, the homogeneous mixture was cast into a custom-made silicone mold with precise dimensions of 35 mm × 15.65 mm × 3 mm. After curing, the specimens were precision-machined to perfectly fit the dimensions of the rectangular waveguide (WR-187 for C-band), ensuring accurate determination of the S-parameters during the VNA measurements. The X-ray diffraction (XRD: Lab 6000) measurement was conducted to analyze the phase composition of the sample. Electrical properties at microwave frequencies of prepared composites were investigated utilizing the transmission / reflection measurement employing a vector network analyzer (MS4642A, 20 GHz). Using a specific calculation (the Nicholson-Ross-Weir method) to turn those measurements (S_{11} and S_{21}) into the complex dielectric constant (ε_r) and loss tangent (tan δ) [15].

3. RESULTS AND DISCUSSION

Fig. 1 shows the x-ray diffraction patterns of zinc tungstate and zinc tungstate with boron oxide powders. The x-ray diffraction analysis of both pure zinc tungstate and zinc tungstate with boron oxide (5 %) composite confirms that both materials exhibit the monoclinic wolframite zinc tungstate phase, consistent with the standard card (no. 96-156-7217). The x-ray diffraction of all specimens corresponds closely with the standard card (no. 96-156-7217) of the monoclinic wolframite $ZnWO_4$ phase [11, 12].

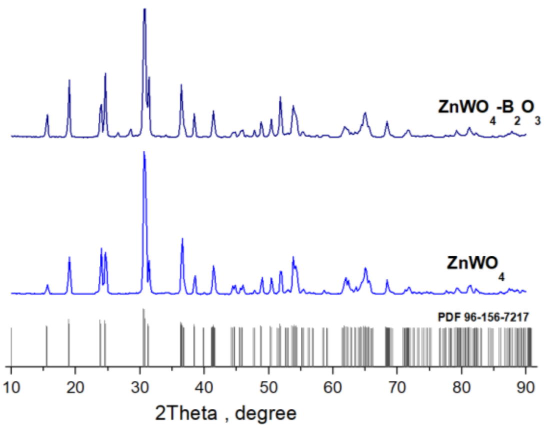

Fig. 1. X-ray Diffraction patterns of zinc tungstate and zinc tungstate-boron oxide

A notable observation is the slight shift in the 2theta values towards higher angles upon the incorporation of boron oxide. This angular shift is indicative of a contraction in the crystal lattice parameters, which consequently results in a reduction in the unit cell volume. Microwave dielectric properties (ε_r and tan δ) of ($ZnWO_4$-B_2O_3) 5 %-epoxy composite in the frequency range of C-band (4 – 8 GHz) were characterized by a Vector Network Analyzer (VNA). As illustrated in Fig. 2. The dielectric constant has relatively stable mean response of 30 with low dispersion in the frequency spectrum measured.

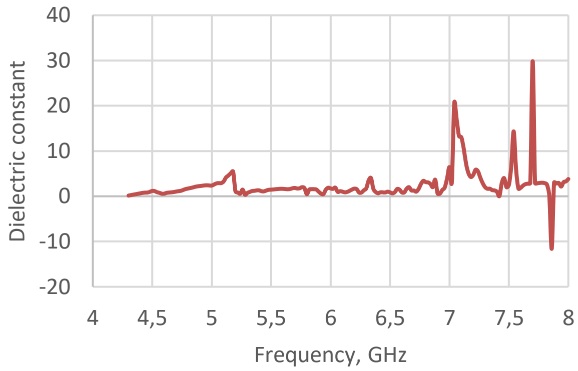

a

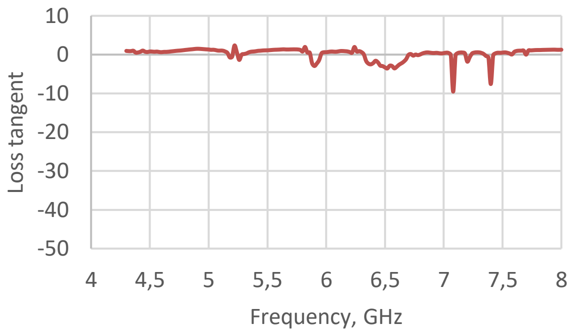

b

Fig. 2. Dielectric properties of zinc tungstate with boron oxide (5 %) composite at frequency rang 4 – 8 GHz: a – dielectric constant of zinc tungstate with boron oxide (5 %) composite; b – loss tangent of zinc tungstate with boron oxide (5 %) composite

At the same time, a low dielectric loss (tan δ) was recorded at 0.0001 For high-performance antennas, the dielectric parameters in terms of frequency independent stability of dielectric parameters and low signal dissipation across the operating bandwidth. As a reference, the dielectric properties of $ZnWO_4$-epoxy composite were characterized to evaluate the impact of B_2O_3 addition. As shown in Fig. 3.

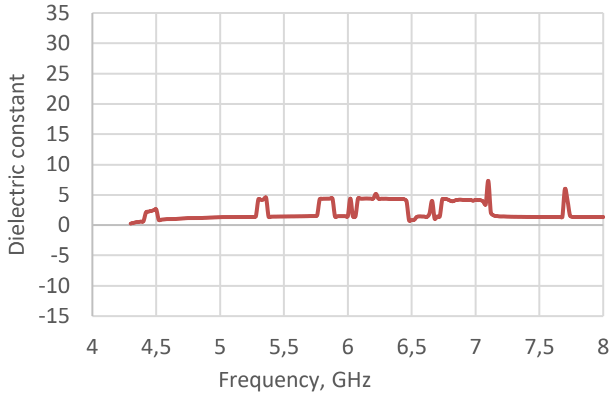

a

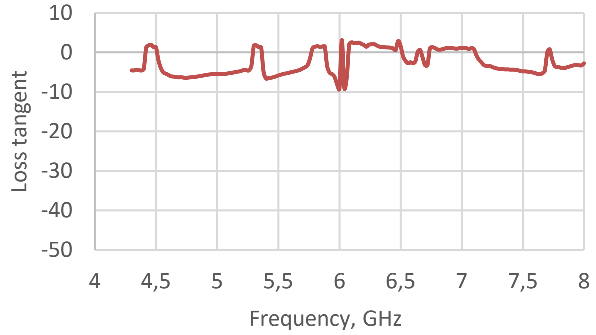

b

Fig. 3. Dielectric properties of zinc tungstate (5 %) composite at frequency rang 4 – 8 GHz: a – dielectric constant of zinc tungstate (5 %) composite; b – loss tangent of zinc tungstate (5 %) composite

The $ZnWO_4$-epoxy composite had lower dielectric constant and slightly higher loss tangent than the B_2O_3 induced zinc tungstate - epoxy composite. The drastic improvement in dielectric constant value of the composites from 5.95 to 30 with incorporation of 5 wt.%B_2O_3 are due to a few synergistic factors. For one, the introduction of boron oxide facilitates the generation of defective sites that serve as charge trapping centers and promote further dipole creation under an external electromagnetic field [12]. The reduction in unit cell volume due to the observed compressive strain (XRD peak shift) may have led to an increased dipole moment density per unit volume [11]. In addition, the grain boundary structure of B_2O_3 enhanced Maxwell-Wagner polarization owing to the concentration of the charge carriers on the polymer-ceramic interfaces [12]. In terms of the dielectric loss, a significant decrease in loss tangent from 0.001 to 0.0001 is primarily attributed to the additional effect of boron oxide on improvement in a stability factor. B_2O_3 limits the movement of free charge carriers, which reduces energy attenuation due to conductance and charge hopping in the composite matrix. Furthermore, the B_2O_3 phase works as an insulating barrier that acts to passivate defect states and oxygen vacancies (which are usually related to high polarization loss) at microwave frequencies. These combined structural and dielectric improvements justify the high radiation efficiency (93.4 %) achieved in the simulated microstrip antenna. Table 1 shows a comparative summary of the dielectric performance of the current study zinc tungstate-5% B_2O_3-epoxy composite against other literature-reported materials.

Table 1. Comparison of dielectric and antenna properties with previous literature

Material system	ε_r	tan δ	Radiation efficiency	Ref.
$ZnWO_4$-5%B_2O_4-epoxy	30	0.0001	93.4%	This study
$ZnWO_4$ ceramics	15.2	0.0020	–	[11]
Li_2CO_3-Al_2O_3-B_2O_3	3.2 – 3.9	–	–	[2]
H_3BO_3 (dry pressing)	2.78 – 2.89	–		[6]
B_2O_3-glass system	12.1	0.0015	–	[12]
5G antenna design	10.2	0.0023	88 %	[13]

3.1. Simulation results for microstrip patch antenna

The simulation of a patch antenna was conducted in CST Studio Suite, using experimental results as input. This was done to evaluate how material properties affect antenna performance and to optimise the dielectric for specific patch antenna applications under study by varying the dielectric material while keeping all other design parameters constant.

3.2. Antenna design and geometry

The antenna was simulated as a rectangular microstrip patch geometry. The substrate was characterized by the measured dielectric properties of the Zinc tungstate-5 wt.% B_2O_3-epoxy composite ($\varepsilon_r = 30$, tan $\delta = 0.0001$) and Zinc tungstate- epoxy composite ($\varepsilon_r = 5.95$, tan δ = 0.001). The size and dimensions of the experimental sample were not changed: 35 mm × 15.65 mm in total surface area with a thickness of 3 mm. From Fig. 4, it was observed according to the parameterized optimization procedure that the patch size resonates with high frequency bands, by benefiting from the high permittivity of the used substrate, something that would not be possible when standard commercial substrates are used.

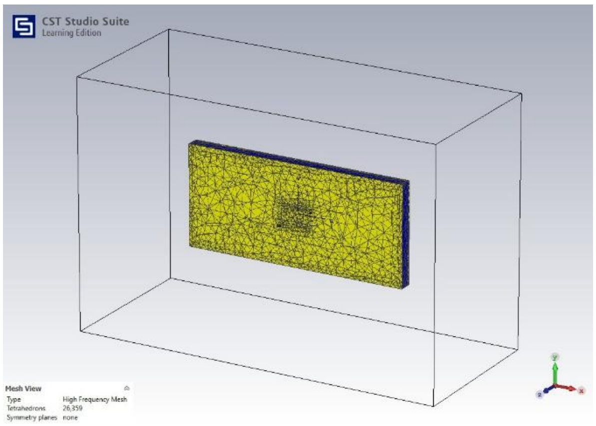

Fig. 4. The simulated antenna design structure (3D perspective view)

3.3. S-parameters analysis

The reflection coefficient S_{11} was analysed for zinc tungstate-epoxy composite and boron oxide-modified composite. to determine resonant frequencies, matching depth, and bandwidth. Fig. 5 a shows dual band response at approximately 6.6 GHz, and 7.7 GHz. S_{11} at resonance approximately -25 dB at 6.6 GHz, and approximately -45 dB at 7.7 GHz. -10 dB bandwidth estimated approximately 0.6 GHz (6.3 – 6.9 GHz) for 6.6 GHZ resonance, and approximately 0.3 GHz (7.5 – 7.8 GHz) for 7.7 GHz resonance.

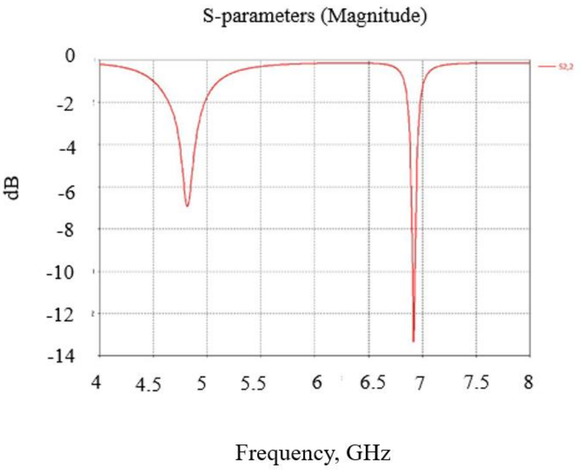

a

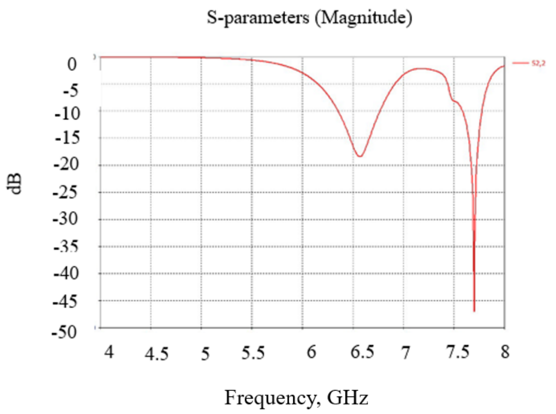

b

Fig. 5. S-parameters from CST Studio Suite: a – S-parameter for zinc tungstate-epoxy composite; b – S-parameter for zinc tungstate-5 wt.% B_2O_3-epoxy composite

S_{11} curve in Fig. 5 b shows dual band response at approximately 4.9 GHz and 7.0 GHz. S_{11} at resonance estimated approximately -7.5 dB at 4.9 GHz and approximately -14 dB at 7.0 GHz. The first resonance at 4.9 GHz does not reach -10 dB no good matching. For the second resonance at 7.0 GHz, the bandwidth is approximately 0.2 GHz (6.9 – 7.1 GHz) S_{11} curve in Fig. 3 b shows that the first resonance is shallow and poorly matched. The second resonance is narrower and deeper, achieving acceptable matching (S11 < -10 dB). Fig. 5 b shown good matching $S_{11} < -10$ dB in both bands. The first is wider and shallower, while the second resonance at 7.7 GHz is narrower and deeper, indicating excellent matching at this frequency.

Boron oxide-modified composite exhibits significantly better performance in terms of matching depth (S_{11} much lower) and bandwidth at the second resonance (7.7 GHz) compared to zinc tungstate-epoxy composite best performance at 7.0 GHz. Additionally, zinc tungstate-5 wt.% B_2O_3-epoxy composite provides two well-operating bands, while zinc tungstate – epoxy composite offers only one acceptable band.

3.4. Voltage standing wave ratio analysis

Fig. 6 shows the Voltage Standing Wave Ratio response (VWSQR) for zinc tungstate-5 wt.% B_2O_3/epoxy composite and zinc tungstate-epoxy composite, respectively. The curve in Fig. 6 a shows an initially very poor match at 4 GHz, with a VSWR of approximately 400.

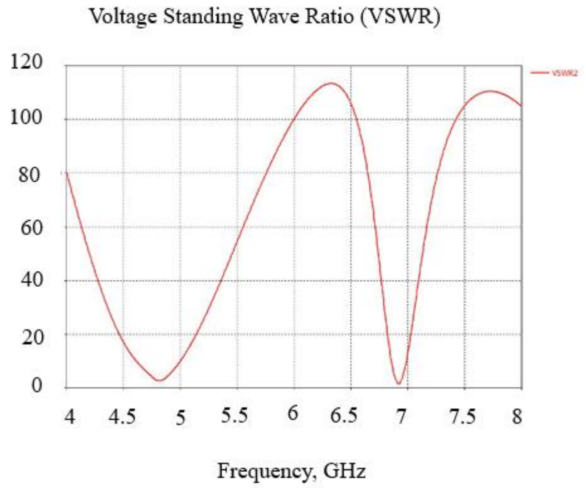

a

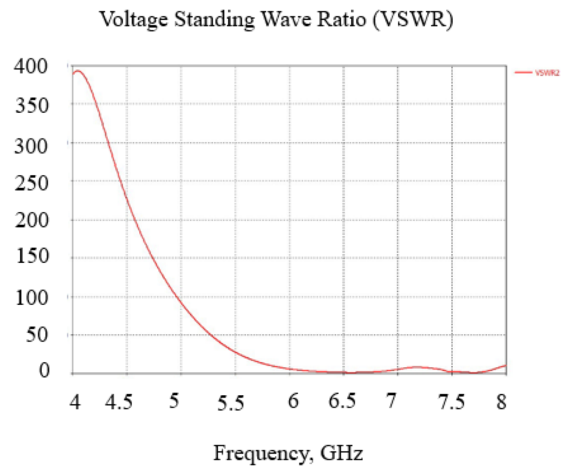

b

Fig. 6. Voltage standing wave ratio from CST Studio Suite: a – far-field for zinc tungstate-epoxy composite; b – far-field for zinc tungstate-5 wt.% B_2O_3-epoxy composite

However, the curve demonstrates a sharp decline, reaching an excellent match near 6.3 GHz where the VSWR approaches 1, followed by a slight rise and then another drop around 7.5 GHz, achieving a VSWR of about 5, which is still considered acceptable.

This behavior results in two relatively wide frequency bands, approximately from 6.0 to 6.7 GHz and from 7.2 to 7.7 GHz, where good impedance matching is maintained, indicating the material’s capability to support multi-band operation with stable matching characteristics across the higher frequency range.

In contrast, Fig.6 b shows a different VSWR response. The VSWR starts at approximately 80 at 4 GHz and decreases toward the first resonance around 4.8 GHz with moderate matching (VSWR ~ 3) but increases sharply, rising to an extremely high value of >100 near 6.3 GHz, followed by a steep drop reaching excellent matching (VSWR nearly equal to one) around the frequency of about 6.9 GHz. Therefore, a limited good matching performance is also available for this material, with the value ranging approximately 6.8 – 7.0 GHz and large VSWR variations over the whole frequency band. Overall, when comparing the two materials, the first offers broader bandwidths with better impedance stability and dual resonances at 6.3 GHz and 7.5 GHz, while the second material, despite achieving a very low VSWR at 6.9 GHz, demonstrates less consistent performance with pronounced variations between resonances. These results highlight the advantage of the first material for applications requiring wider operational bandwidth and more stable matching behavior.

3.5. Far-field and near-field analysis

The electromagnetic performance of the patch antenna employing the two investigated dielectric materials was evaluated at 7.74 GHz. Zinc tungstate-5 wt.% B_2O_3-epoxy composite demonstrated superior characteristics, with a radiation efficiency of approximately 93.4 % and a total efficiency of 90.5 %. Its directivity attained a 5.06 dBi, with remarkable side lobe attenuation of around -11.7 dB in the Phi = 0 plane, despite performance modulated across planes, exhibiting a broader beamwidth and reduced gain in the Phi = 90 plane. The radiation patterns were primarily directive along the positive z-axis, as shown in Fig. 7.

In contrast, the zinc tungstate-epoxy composite exhibited lower efficiencies, with a radiation efficiency of approximately 75.1 % and total efficiency reduced to about 2.7 %, largely due to its higher loss tangent and operation outside its optimal resonance near 7.0 GHz. The maximum directivity was approximately 3.1 dBi, and the radiation patterns maintained stable dipole-like figure-eight shapes across a wide frequency range from 5 to 8 GHz, reflecting high pattern consistency but limited directivity and side lobe control, as shown in Fig. 8. These results indicate that zinc tungstate-5 wt.% B_2O_3-epoxy composite is more suitable for applications requiring high efficiency, directivity, and good impedance matching at targeted frequencies, while zinc tungstate-epoxy composite may be considered for scenarios prioritising stable radiation characteristics over broader frequency ranges, albeit with lower efficiency and matching performance. All results of the simulation are shown in Table 1. These results also suggest that the use of zinc tungstate-5 wt.%B_2O_3-epoxy composite is better for high efficiency, directivity and good impedance matching at the desired frequency ranges whereas zinc tungstate-epoxy composite may be suited to applications demand for stable radiation characteristics in a frequency range due to low efficiency and matching performance. The physical parameters of the synthesized composite were used to simulate the microstrip patch antenna: length: 35 mm; width: 15.65 mm; thickness: 3 mm.

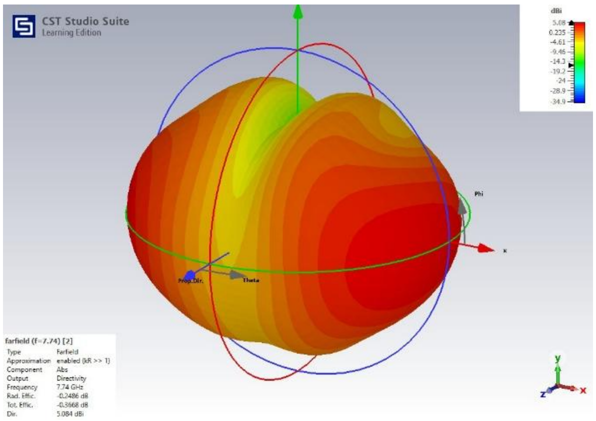

a

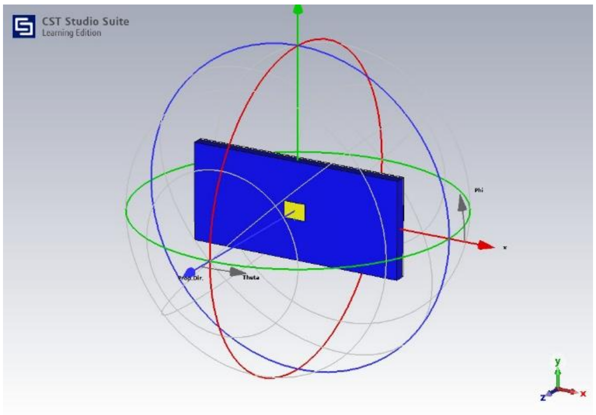

b

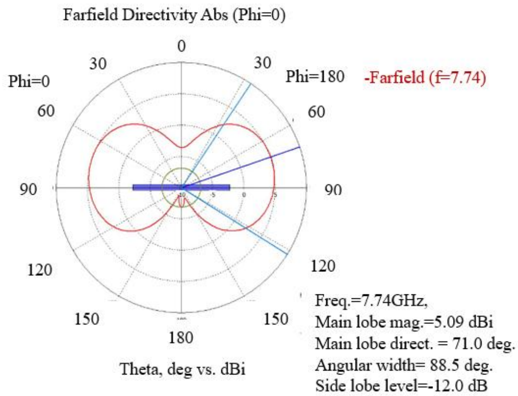

c

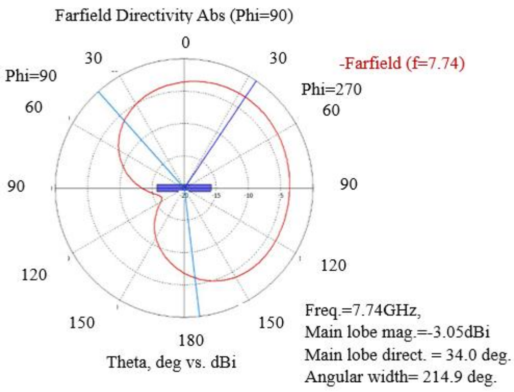

d

continued on the next page

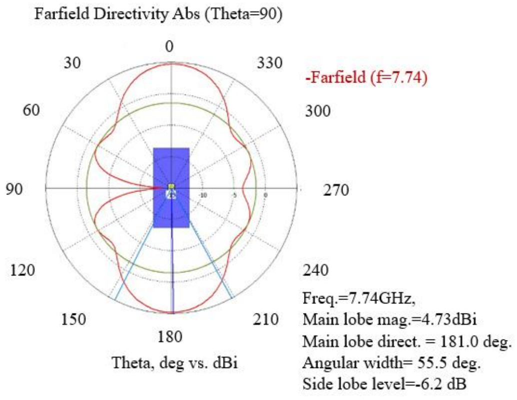

e

Fig. 7. Far-field and near-field from CST Studio Suite zinc tungstate-5 wt.% B_2O_3-epoxy composite: a – 3D radiation pattern shows the total realized gain of the microstrip antenna at 7.74 GHz; b – geometric configuration and design parameters of microstrip antenna; c – radiation pattern depicted in cartesian coordinates at resonance frequency; d – polar radiation pattern (E plane and H plane) of microstrip antenna at 7.74 GHz; e – surface current distribution on microstrip antenna at resonance frequency

These dimensions were employed in the CST studio suite so that the simulation could represent the real situation of zinc tungstate-5 wt.% B_2O_3-epoxy. ε_r of 30 together with the optimal thickness of 3 mm contributed to in a highly miniaturized and efficient radiator, achieving a return loss S_{11} of -45 dB at 7.7 GHz.

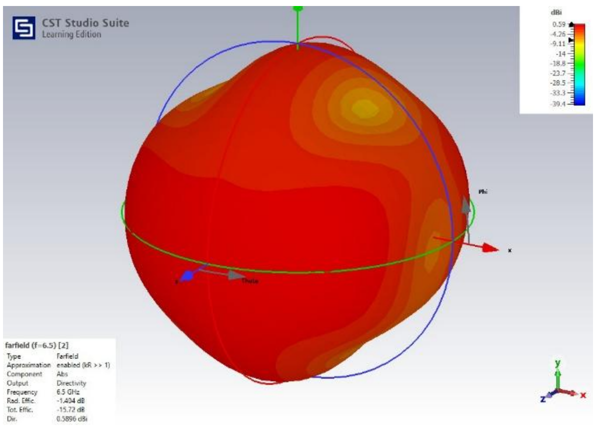

a

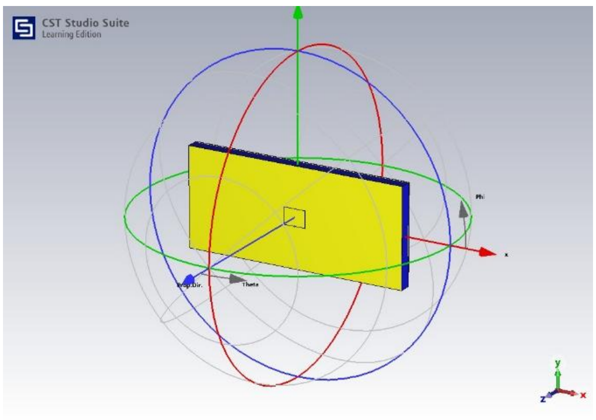

b

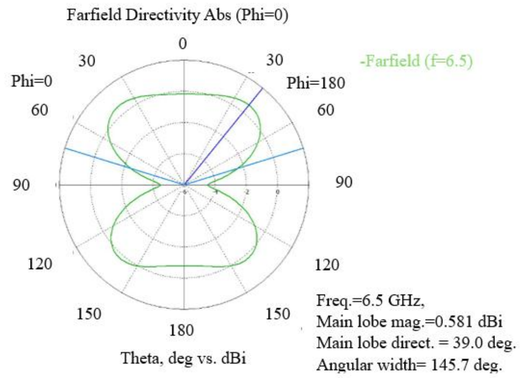

c

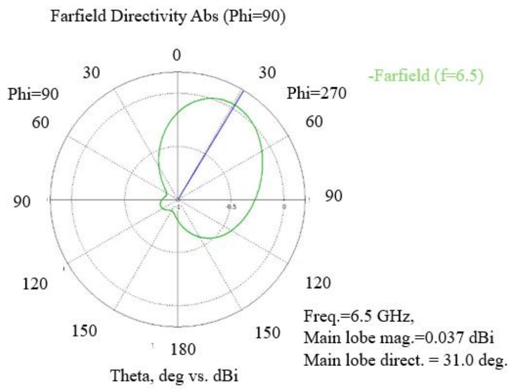

d

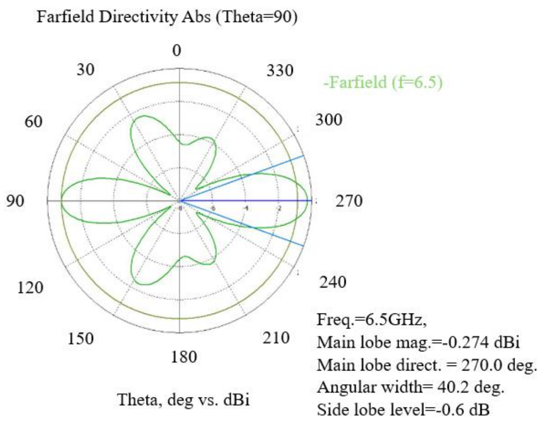

e

Fig. 8. Far-field and near-field from CST studio suite for zinc tungstate-epoxy composite: a – 3D radiation pattern shows the total realized gain of the microstrip antenna at 6.5 GHz; b – geometric configuration and design parameters of microstrip antenna; c – radiation pattern depicted in cartesian coordinates at resonance frequency; d – polar radiation pattern (E plane and H plane) of microstrip antenna at 6.5 GHz; e – surface current distribution on microstrip antenna at resonance frequency

The achieved radiation efficiency of 93.4 % and the return loss of -45.16 dBi at 7.7 GHz demonstrate that this composite is highly efficient for 5 G applications. These performance metrics surpass the dual-substrate antenna configurations recently proposed by Al-Azzawi [13], highlighting the advantage of using boron oxide induced zinc tungstate as a high-permittivity substrate. These findings are in line with the hypothesized concordance and the working hypothesis of this study. The good enhancement in the dielectric and radiation properties with 5 wt.% boron oxide is also consistent with previous work [11, 12], where boron oxide is a densifier and stabilizer of the composite network. In particular, the obtained radiation efficiency of 93.4 % and return loss of -45.16 dB at 7.7 GHz validate that optimization of the ceramic-fille rmay result in better performances of the antenna, achieving performances higher than those reported for similar frequency applications [13]. All results of the simulation are shown in Table 2.

Table 2. Results of the simulation for microstrip patch antenna

Parameter	$ZnWO_4$-epoxy	$ZnWO_4$-5 % B_2O_3-epoxy	
Resonant frequencies	4.9 and 7.0	6.6 and 7.7	
Reflection coefficient S_{11}, dB	-7.5 and -14	-25 and -45	
-10 dB bandwidth, GHz	0.2 (at 7.0 GHz)	0.6 and 0.3	
Radiation efficiency, %		75.1 %	93.4 %
Total efficiency, %		2.7 %	90.5 %
Directivity, dBi		3.1	5.06
VSWR at eesonance		~1	~1

4. CONCLUSIONS

In this work, the influence of B_2O_3 addition on the structure, dielectric properties, and microwave absorption properties of zinc tungstate-epoxy composite has been studied systematically. The XRD result revealed the realisation of the zinc tungstate phase with the increase of 5 wt.% B_2O_3, resulting in a pronounced improvement of the dielectric properties. In particular, the relative permittivity increased up to 30, while the dielectric loss decreased down to 0.0001, indicating excellent energy storage capability with minimal dissipation. The dielectric properties were experimentally measured over the C-band frequency range (4 – 8 GHz), where a significant enhancement was observed at the resonant frequency of 7.7 GHz.

The practical application of the fabricated composite is also demonstrated by CST Studio Suite simulations for a patch antenna. The zinc tungstate-5 wt.% B_2O_3 composite exhibited outstanding antenna properties; dual-band response was observed with an ultra-deep matching depth (S_{11}) of -45 dB and a high radiation efficiency of 93.4 %. These data are better than the pure zinc tungstate-epoxy composite, which showed low efficiency (75.1 %) and bad impedance matching. In summary, it can be concluded that the zinc tungstate-5 wt.% B_2O_3/epoxy composite is a high-performance, low-cost and ideal substrate material for the above modern wireless communication systems as well as frequency-selective device applications [16]. The results successfully support the working hypothesis that incorporating boron oxide into the zinc tungstate-epoxy matrix creates a synergistic effect that optimizes both electrical and radiation performance, offering a superior alternative to traditional microwave substrates.

REFERENCES

1. **Sun, J.S.** Microwave Dielectric Materials for Wireless Communication *Journal of Advanced Ceramics* 12 (3) 2021: pp. 450 – 465. https://doi.org/10.1007/s40145-020-0441-2
2. **Wang, H., Zhang, X., Li, L., Liu, X., Chen, R.** Low-Temperature Sintering and Microwave Dielectric Properties of Li_2CO_3-Al_2O_3-B_2O_3 Ceramics. *Journal Of the European Ceramic Society* 35 (4) 2015: pp. 1205 – 1212. https://doi.org/10.1016/j.jeurceramsoc.2014.10.035
3. **Zhou, X., Pang, D., Ding, L.** Sintering Behavior and Microwave Dielectric Properties of Bi_2O_3-H_3BO_3 Doped Ceramic Systems *Ceramics International* 42 (8) 2016: pp. 9845 – 9852 https://doi.org/10.1016/j.ceramint.2016.03.078
4. **Zhou, Y., Li, C.** Low-Temperature Sintering of CuO-ZnO-B_2O_3-Li_2O/Al_2O_3 Composites for ULTCC Applications *Journal of Materials Science: Materials in Electronics* 28 (15) 2017: pp. 11234 – 11241. https://doi.org/10.1007/s10854-017-6913-4
5. **Pang, M., Ding, H., Li, S.** Low-Temperature Dehydration Synthesis and Microwave Dielectric Properties of HBO_2 Ceramics *Materials Letters* 190 2017: pp. 154 – 157. https://doi.org/10.1016/j.matlet.2016.12.115
6. **Ding, H., Li, M., Zhang, P., Wang, J., Sun, Q., Xu, J.** High-Performance H_3BO_3 Ceramics Prepared by Room-Temperature Dry Pressing *Journal of The American Ceramic Society* 101 (5) 2018: pp. 2100 – 2108. https://doi.org/10.1111/jace.15366
7. **Li, S., Wang, Y., Zhao, T., Müller, R., Schmidt, H.** Cold Sintering and Moisture Absorption Challenges in Borate-Based Microwave Ceramics *Journal of Alloys and Compounds* 780 2019: pp. 850 – 858. https://doi.org/10.1016/j.jallcom.2018.12.016
8. **Bi, K., Ma, J., Luo, W., Gong, M.** Magnetoelectric Properties of Polymer-Based Ceramic Composites *Materials Chemistry and Physics* 212 2018: pp. 314 – 320. https://doi.org/10.1016/j.matchemphys.2018.03.056
9. **Hu, T., Ju, C., Chen, R., He, Y.** Dielectric Properties of $ZnWO_4$-epoxy Composites for Microwave Applications *Journal of Materials Research* 34 (12) 2019: pp. 2015 – 2022. https://doi.org/10.1557/jmr.2019.123
10. **Zuo, R., Fu, J., Shi, M., Qi, H.** Development of Low-Loss Microwave Dielectric Ceramics For 5G Technology *Journal of Advanced Dielectrics* 10 (2) 2020: pp. 2050011. https://doi.org/10.1142/S201013252050011X
11. **Kumar, S., Yadav, R.P.** Structural, Morphological and Microwave Dielectric Studies on Microwave Sintered $ZnWO_4$ Ceramic Compounds *Journal of Materials Science: Materials in Electronics* 34 (14) 2023: pp. 1150 – 1162. https://doi.org/10.1007/s10854-023-10543-y
12. **Zhao, L., Wang, X., Liu, Y.** The Effect of Boron Anomaly on The Dielectric Properties and Stability of Composite Systems *Ceramics International* 50 (2) 2024: pp. 3412 – 3420. https://doi.org/10.1016/j.ceramint.2023.11.102
13. **Al-Azzawi, M.A.** High-Performance Microstrip Patch Antenna Using Dual-Substrate Configuration For 5G *IEEE Antennas and Wireless Propagation Letters* 23 (1) 2024: pp. 88 – 92. https://doi.org/10.1109/LAWP.2023.3321528
14. **Nicolson, A.M., Ross, G.F.** Measurement of The Intrinsic Properties of Materials by Time-Domain Techniques *IEEE*

Transactions on Instrumentation and Measurement 19 (4) 1970: pp. 377 – 382. https://doi.org/10.1109/TIM.1970.4313932

15. **CST Studio Suite.** Electromagnetic Field Simulation Software, Dassault Systèmes. Accessed January 2026. https://www.3ds.com/products-services/simulia/products/cst-studio-suite/

16. **Williams, K.J.** Advancements in Grain Boundary Engineering for Zinc-Based Microwave Ceramics *Advanced Functional Materials* 34 (8) 2024: pp. 2304551. https://doi.org/10.1002/adfm.202304551